

Continual learning-based probabilistic slow feature analysis for multimode dynamic process monitoring

Jingxin Zhang, Donghua Zhou, *Fellow, IEEE*, and Maoyin Chen, *Member, IEEE*, Xia Hong, *Senior Member, IEEE*

Abstract—In this paper, a novel multimode dynamic process monitoring approach is proposed by extending elastic weight consolidation (EWC) to probabilistic slow feature analysis (PSFA) in order to extract multimode slow features for online monitoring. EWC was originally introduced in the setting of machine learning of sequential multi-tasks with the aim of avoiding catastrophic forgetting issue, which equally poses as a major challenge in multimode dynamic process monitoring. When a new mode arrives, a set of data should be collected so that this mode can be identified by PSFA and prior knowledge. Then, a regularization term is introduced to prevent new data from significantly interfering with the learned knowledge, where the parameter importance measures are estimated. The proposed method is denoted as PSFA-EWC, which is updated continually and capable of achieving excellent performance for successive modes. Different from traditional multimode monitoring algorithms, PSFA-EWC furnishes backward and forward transfer ability. The significant features of previous modes are retained while consolidating new information, which may contribute to learning new relevant modes. Compared with several known methods, the effectiveness of the proposed method is demonstrated via a continuous stirred tank heater and a practical coal pulverizing system.

Index Terms—Multimode dynamic process monitoring, probabilistic slow feature analysis, elastic weight consolidation, continual learning ability

I. INTRODUCTION

Data-driven process monitoring is vitally important for ensuring safety and reliability of modern industrial processes [1]–[3]. Dynamic process monitoring methods have been extensively studied in recent years [4]–[6]. The slow feature analysis (SFA), which is effective in extracting invariant slow features from fast changing sensing data [7], has been widely extended to process monitoring applications. It is shown that SFA can be applied to establish a comprehensive operating status, where the nominal operating deviations and the real faults may be distinguished in the closed-loop systems [8]–[12]. Recursive SFA (RSFA) [9] and recursive exponential

SFA [10] were developed and the associated parameters were updated for adaptive monitoring. Sufficient samples had been required to establish the initial model when a new mode was identified. Probabilistic SFA (PSFA) was proposed as a probabilistic framework for dynamic processes [11], [13] with the advantage of effectively handling process noise and uncertainties, in which measurement noise was modeled and missing data could be settled conveniently [12].

Most industrial systems operate in multiple operating conditions due to equipment maintenance, market demands, changing of raw materials, etc. Multimode dynamic process monitoring approaches have been widely investigated, which currently can be sorted into two broad categories [14], namely, single-model schemes and multiple-model methods. Single-model methods transform the multimode data to unimodal distribution [15], [16] or establish the adaptive models. Local neighborhood standardization can normalize data into the same distribution and popular methods for one mode could be applied [15]. However, the effectiveness may be influenced by the matching degree of training and testing samples. Recursive principal component analysis was adopted for adaptive process monitoring [17]. Although prior knowledge is not required, these algorithms are effective for slow changing features and may fail to track the dramatic variations on the entire dataset.

The mainstream approaches of multimode monitoring are based on multiple-model schemes, where the modes are identified and the local models are established within each mode. Mixture of canonical variate analysis (MCVA) was explored and the mode was identified by Gaussian mixture models [18]. Improved mixture of probabilistic principal component analysis (IMPPCA) could be utilized for multimode processes [1], where the monitoring model parameters and the mode identification parameters were jointly optimized. Generally, the number of modes is a priori and data from all possible modes are required before learning, which is infeasible and time-consuming [14]. When novel modes appear, sufficient data should be collected and new local models are relearned correspondingly. The monitoring model is only effective for the learned modes, but may be difficult to deliver excellent performance for similar modes. Multiple-model schemes seem to be redundant and difficult to identify modes accurately [19]. Furthermore, the model's capacity and storage costs increase significantly with the emergence of modes.

Recently, the emergent research area of continual learning has received much attention in machine learning [20]–[24]. It concerns the modeling of sequential tasks with the knowledge being acquired continually, fine-tuned and transferred through-

This work was supported by National Natural Science Foundation of China [grant numbers 62033008, 61873143]. (Corresponding authors: Donghua Zhou; Maoyin Chen)

Jingxin Zhang and Maoyin Chen are with the Department of Automation, Tsinghua University, Beijing 100084, China (e-mail: zjx18@mails.tsinghua.edu.cn; mychen@tsinghua.edu.cn).

Donghua Zhou is with College of Electrical Engineering and Automation, Shandong University of Science and Technology, Qingdao 266000, China and also with the Department of Automation, Tsinghua University, Beijing 100084, China (e-mail: zdh@mail.tsinghua.edu.cn).

Xia Hong is with Department of Computer Science, School of Mathematical, Physical and Computational Sciences, University of Reading, RG6 6AY, U.K.

This paper has been submitted to IEEE Transactions on Cybernetics for potential publication.

out the entire learning process [25]. Continual adaptation to the changing tasks is achieved by acquiring new information while preserving the learned knowledge. One long-standing challenge to be addressed is catastrophic forgetting issue, namely, learning a model with new information would influence the previously learned knowledge [26]. Current continual learning-based algorithms focus on the image processing and generally require the class labels [20]–[26]. One of the continual learning paradigms is called elastic weight consolidation (EWC) [20], in which it is analyzed that when a full data set of multiple tasks are decomposed based on a sequence of incoming tasks, the model parameter can be adjusted accordingly based on data from a new task, without sacrificing performance for any previously learned tasks.

Similarly, in the context of multimode process monitoring, new modes would often appear continuously and different modes may share the similar significant features [19]. In practical applications, it is often intractable to collect data from all modes. Zhang *et al.* applied continual learning into multimode process monitoring [27], where EWC was employed to settle the catastrophic forgetting of principal component analysis (PCA), referred to as PCA-EWC. However, data are static in each mode and the mode has to be identified by statistical characteristics of data, which makes it ineffective for multimode dynamic processes, as well as difficult to distinguish the operating deviations and dynamic anomalies.

Against this background, this paper considers continual learning by extending EWC to PSFA, which is regarded as underlying multimode dynamic processes for the observed sequential data. The proposed method is referred to as PSFA-EWC. Data from each mode arrive sequentially and unknown modes are allowed. Moreover, the proposed algorithm would be best to distinguish the real faults and the normal operating derivations. When a new mode is identified by PSFA and prior knowledge, it is assumed that a set of data are collected before learning. A quadratic penalty term is introduced to avoid the dramatic changes of mode-relevant parameters when a new mode is trained [28]. Similar to [27], EWC is adopted to estimate the PSFA model parameter importance. The information from novel modes is assimilated while consolidating the learned knowledge simultaneously, thus delivering continual learning ability for successive modes.

The contributions are summarized as follows:

- a) Continual learning based PSFA is firstly investigated for multimode dynamic processes, where the mode is identified by the monitoring statistic and expert experience.
- b) The previously learned knowledge is retained while consolidating new information, which may aid the learning of future relevant modes. Thus, PSFA-EWC furnishes the forward and backward transfer ability.
- c) Within the probabilistic framework, PSFA-EWC could provide excellent interpretability, and can deal with missing data, measurement noise and uncertainty.

The rest of this paper is organized below. Section II reviews PSFA and EWC succinctly and outlines the basic idea of our proposed approach. The technical core of PSFA-EWC is detailed in Section III. The monitoring procedure and comparative experiments are designed in Section IV. The

effectiveness of PSFA-EWC are illustrated by a continuous stirred tank heater (CSTH) and a practical coal pulverizing system in Section V. The conclusion is given in Section VI.

II. PRELIMINARIES

For ease of exposition, we start with introducing the PSFA for a single mode, since it serves as basic ingredient of our proposed multimode PSFA. Then the basic idea of EWC as well as how to extend EWC to multimode PSFA is outlined.

A. PSFA for a single mode

In the probabilistic framework of SFA, the objective is to identify the slowest varying latent features from a sequence of time-varying observations $\mathbf{x}_t \in R^m$, $t = 1, 2, \dots, T$, which can be represented/generated via a state-space model [13] with a first-order Markov chain architecture [11], [29].

$$\begin{aligned} \mathbf{x}_t &= \mathbf{V} \mathbf{y}_t + \mathbf{e}_t, & \mathbf{e}_t &\sim N(\mathbf{0}, \Sigma_x) \\ \mathbf{y}_t &= \Lambda \mathbf{y}_{t-1} + \mathbf{w}_t, & \mathbf{w}_t &\sim N(\mathbf{0}, \Sigma) \\ \mathbf{y}_1 &= \mathbf{u}, & \mathbf{u} &\sim N(\mathbf{0}, \Sigma_1) \end{aligned} \quad (1)$$

where the low dimensional latent variable $\mathbf{y}_t \in R^p$, $p < m$. $\Lambda = \text{diag}(\lambda_1, \dots, \lambda_p)$, with the constraint $\Lambda^2 + \Sigma = \mathbf{I}$ to ensure the covariance matrix be the unit matrix \mathbf{I} . The emission matrix is $\mathbf{V} \in R^{m \times q}$ and measurement noise variance is $\Sigma_x = \text{diag}(\sigma_1^2, \dots, \sigma_m^2)$.

For a single mode, the observed data and latent slow features sequences are denoted as $\mathbf{X}_s = \{\mathbf{x}_t\} \in R^{m \times T}$ and $\mathbf{Y}_s = \{\mathbf{y}_t\} \in R^{p \times T}$, respectively. T is the number of samples and the estimation of p has been discussed in [12].

The joint distribution is given as [13]

$$P(\mathbf{X}_s | \mathbf{Y}_s) = P(\mathbf{y}_1) \prod_{t=2}^T P(\mathbf{y}_t | \mathbf{y}_{t-1}) \prod_{t=1}^T P(\mathbf{x}_t | \mathbf{y}_t) \quad (2)$$

Let $\theta_x = \{\mathbf{V}, \Sigma_x\}$, $\theta_y = \{\Sigma_1, \Lambda\}$. The objective of PSFA is to estimate parameters $\theta = \{\theta_x, \theta_y\}$ by maximizing the complete log likelihood function:

$$\begin{aligned} \log P(\mathbf{X}_s, \mathbf{Y}_s | \theta) &= \sum_{t=1}^T \log P(\mathbf{x}_t | \mathbf{y}_t, \theta_x) + \log P(\mathbf{y}_1 | \Sigma_1) \\ &\quad + \sum_{t=2}^T \log P(\mathbf{y}_t | \mathbf{y}_{t-1}, \Lambda) \end{aligned} \quad (3)$$

According to (1), (3) is reformulated as

$$\begin{aligned} &\log P(\mathbf{X}_s, \mathbf{Y}_s | \theta) \\ &= -\frac{1}{2} \left\{ (m+p)T \log 2\pi + (T-1) \log |\Sigma| + \mathbf{y}_1^T \Sigma_1^{-1} \mathbf{y}_1 \right. \\ &\quad \left. + T \log |\Sigma_x| + \sum_{t=1}^T (\mathbf{x}_t - \mathbf{V} \mathbf{y}_t)^T \Sigma_x^{-1} (\mathbf{x}_t - \mathbf{V} \mathbf{y}_t) \right. \\ &\quad \left. + \log |\Sigma_1| + \sum_{i=2}^T (\mathbf{y}_i - \Lambda \mathbf{y}_{i-1})^T \Sigma^{-1} (\mathbf{y}_i - \Lambda \mathbf{y}_{i-1}) \right\} \end{aligned} \quad (4)$$

The optimal parameter θ is optimized by maximizing (4) using expectation maximization (EM) algorithm [30].

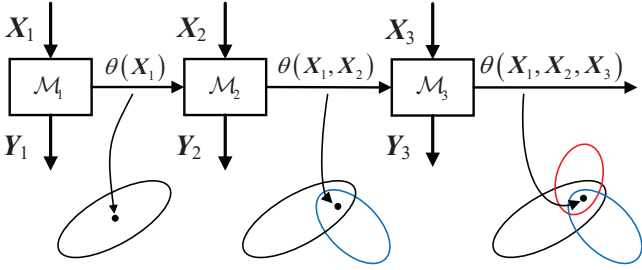


Fig. 1. An illustration of the proposed PSFA-EWC with continual learning ability for three consecutive modes $\mathcal{M}_1, \mathcal{M}_2, \mathcal{M}_3$.

B. Elastic weight consolidation for multimode PSFA

In the following we explain the basic idea of extending EWC for multimode PSFA processes and then summarize the key objectives of proposed PSFA-EWC. Consider also based on PSFA model (1), in the multimode scenario where data stream are generated as incoming new modes \mathcal{M}_K , $K = 1, 2, \dots$ one at a time. For each mode \mathcal{M}_K , normal data $\mathbf{X}_K \in R^{m \times T_K}$ are collected, where T_K is the number of samples. Correspondingly it is assumed that $\mathbf{Y}_K \in R^{p \times T_K}$ need to be extracted from the K th mode. Denote the total observed data and its latent slow features as $\mathbf{X} = \{\mathbf{X}_1, \mathbf{X}_2, \dots\}$, $\mathbf{Y} = \{\mathbf{Y}_1, \mathbf{Y}_2, \dots\}$.

EWC initially considers the use of Bayesian rule for the sequential learning process in which the most probable parameters should be found by maximizing the conditional probability [20]

$$\log P(\theta|\mathbf{X}, \mathbf{Y}) = \log P(\mathbf{X}, \mathbf{Y}|\theta) + \log P(\theta) - \log P(\mathbf{X}, \mathbf{Y}) \quad (5)$$

where $P(\theta)$ is prior probability and $P(\mathbf{X}, \mathbf{Y}|\theta)$ is the data probability. For illustration only the first two successive independent modes \mathcal{M}_1 and \mathcal{M}_2 are initially considered. Then, (5) can be reformulated as [20]:

$$\log P(\theta|\mathbf{X}, \mathbf{Y}) = \log P(\mathbf{X}_2, \mathbf{Y}_2|\theta) + \log P(\theta|\mathbf{X}_1, \mathbf{Y}_1) + \text{don't care terms} \quad (6)$$

where $\log P(\theta|\mathbf{X}, \mathbf{Y})$ is the posterior probability of the parameter given the entire dataset. $\log P(\mathbf{X}_2, \mathbf{Y}_2|\theta)$ represents the loss function for mode \mathcal{M}_2 . Posterior distribution $\log P(\theta|\mathbf{X}_1, \mathbf{Y}_1)$ can reflect all information of mode \mathcal{M}_1 [20], [27]. This equation reflects the key idea of EWC in continual learning framework of updating system parameters based on a composite cost function that is dependent on current parameters learned from previous data and new incoming data by using posterior distribution $\log P(\theta|\mathbf{X}_1, \mathbf{Y}_1)$ which acts as a constraint in future objective, so that the learned knowledge will not be forgotten.

Note that this is the first time that EWC is extended to PSFA for monitoring in which new optimization procedures of proposed PSFA-EWC algorithm will be introduced in Section III, as illustrated in Fig. 1 for three modes. The multimode slow features for each mode are extracted, while the model parameter θ is continually updated using only data of a new mode, while maintaining performance of all old modes. Black,

blue and red circles represent the optimal parameter regions that the log likelihoods for modes $\mathcal{M}_1, \mathcal{M}_2$ and \mathcal{M}_3 are maximized, respectively. This process can be generalized to $K > 3$ modes, with

$$\log P(\theta|\mathbf{X}, \mathbf{Y}) = \log P(\mathbf{X}_K, \mathbf{Y}_K|\theta) + \log P(\theta|\mathcal{M}_{i=1}^{K-1}) + \text{don't care terms} \quad (7)$$

where $P(\theta|\mathcal{M}_{i=1}^{K-1}) \triangleq P(\theta|\mathbf{X}_1, \dots, \mathbf{X}_{K-1}, \mathbf{Y}_1, \dots, \mathbf{Y}_{K-1})$.

Note that the first term in (7) is complete likelihood for K th mode. The second term in (7) is parameter estimate that reflects information from all previous modes, thus can be interpreted as log prior probability of parameter for K th mode. Since it is assumed that data from all previous modes will not be accessible to obtain $P(\theta|\mathcal{M}_{i=1}^{K-1})$ exactly, it is found by recursive approximation as detailed in Section III-A.

III. THE PROPOSED PSFA-EWC ALGORITHM

A. Recursive Laplacian approximation of $P(\theta|\mathcal{M}_{i=1}^{K-1})$

Consider the multimode PSFA process where data are collected sequentially with mode index $K = 1, 2, 3, \dots$. For the sake of notational simplicity, it is assumed in the sequel that the data \mathbf{x}_t and corresponding slow features \mathbf{y}_t start from $t = 1$ at the beginning and end at $t = T_K$ of the K th mode. The proposed PSFA-EWC algorithm starts with solving an initial single mode model as $K = 1$. It is initially assumed that an optimal parameter, denoted as $\theta_{\mathcal{M}_1}^*$, has been obtained from the first mode \mathcal{M}_1 based on solving (4). For later modes ($K \geq 2$), the monitoring model is updated recursively based on the data from K th mode and the current monitoring model before K , where EM is employed [30] to solve the optimization problem of maximizing $J(\theta)$ in Section III-B.

Specifically consider initially the case of two modes $K = 2$, then the term $\log P(\theta|\mathcal{M}_1)$ in (7) is approximated by the Laplace approximation [20], [27] as

$$\log P(\theta|\mathcal{M}_1) \approx -\frac{1}{2}(\theta - \theta_{\mathcal{M}_1}^*)^T (T_1 \mathbf{F}(\theta_{\mathcal{M}_1}^*) + \lambda_{\text{prior}} \mathbf{I}) \cdot (\theta - \theta_{\mathcal{M}_1}^*) + \text{constant}$$

where $\mathbf{F}(\theta_{\mathcal{M}_1}^*)$ is Fisher information matrix (FIM) and computed by (26) in Appendix A. $\lambda_{\text{prior}} \mathbf{I}$ is the Gaussian prior precision matrix for mode \mathcal{M}_1 . However, the sample size would have non-negligible influence on the approximation. To ensure the approximation quality, a mode-specific hyperparameter $\eta_1 > 0$ is introduced to replace T_1 [31], namely,

$$\log P(\theta|\mathcal{M}_1) = -\frac{1}{2}(\theta - \theta_{\mathcal{M}_1}^*)^T \boldsymbol{\Omega}_{\mathcal{M}_1} (\theta - \theta_{\mathcal{M}_1}^*) + \text{constant}$$

where $\boldsymbol{\Omega}_{\mathcal{M}_1} = \eta_1 \mathbf{F}(\theta_{\mathcal{M}_1}^*) + \lambda_{\text{prior}} \mathbf{I}$.

Then the K th mode \mathcal{M}_K arrives ($K \geq 3$), we approximate $P(\theta|\mathcal{M}_{i=1}^{K-1})$ by recursive Laplace approximation [27] as

$$\log P(\theta|\mathcal{M}_{i=1}^{K-1}) \approx -\frac{1}{2}(\theta - \theta_{\mathcal{M}_{K-1}}^*)^T \boldsymbol{\Omega}_{\mathcal{M}_{K-1}} (\theta - \theta_{\mathcal{M}_{K-1}}^*) + \text{constant}$$

where

$$\boldsymbol{\Omega}_{\mathcal{M}_{K-1}} = \boldsymbol{\Omega}_{\mathcal{M}_{K-2}} + \eta_{K-1} \mathbf{F}_{\mathcal{M}_{K-1}}, \quad K \geq 3 \quad (8)$$

Note that $\mathbf{F}_{\mathcal{M}_{K-1}}$ is FIM of mode \mathcal{M}_{K-1} , and η_{K-1} is the hyperparameter. Thus $P(\theta|\mathcal{M}_{i=1}^{K-1})$ is approximated by a quadratic term centered at current optimum, with weighting $\Omega_{\mathcal{M}_{K-1}}$ acting as an importance measure regulating data from all previous $K-1$ modes.

Specifically when K th mode has been learned (see PSFA-EWC algorithm in Section III-B), the importance measures specific to PSFA are updated and ready as $(K+1)$ th mode.

$$\Omega_{\mathcal{M}_K}^V = \Omega_{\mathcal{M}_{K-1}}^V + \eta_K^V \mathbf{F}_{\mathcal{M}_K}^V \quad (9)$$

$$\Omega_{\mathcal{M}_K}^\Lambda = \Omega_{\mathcal{M}_{K-1}}^\Lambda + \eta_K^\Lambda \mathbf{F}_{\mathcal{M}_K}^\Lambda \quad (10)$$

where $\mathbf{F}_{\mathcal{M}_K}^V$ and $\mathbf{F}_{\mathcal{M}_K}^\Lambda$ are FIMs and calculated in Appendix A. η_K^V and η_K^Λ are mode-specific hyperparameters. Similar to [20], η_K^V and η_K^Λ are optimized by hyperparameter search and fined-tune by prior knowledge, which may play an important role in accurate estimate of probability with sequential modes. Actually, it's a parameter redistribution from equal importance since previous modes would be counted more than recent ones in recursion. Large values of η_K^V and η_K^Λ indicate that the K th mode is significant and the weight of previous modes decreases. Small values mean that we expect to acquire better performance of previous modes by sacrificing the performance of current mode. In this case, it has been concluded by prior knowledge that the current mode may be unimportant and needs to be forgotten gracefully.

B. PSFA-EWC algorithm

Consider the objective of PSFA-EWC of maximizing

$$J(\theta) = \log P(\mathbf{X}_K, \mathbf{Y}_K|\theta) + \log P(\theta|\mathcal{M}_{i=1}^{K-1}) \quad (11)$$

subject to PFSA model (1). Recall (3), the log-likelihood function for the current mode \mathcal{M}_K is represented by

$$\begin{aligned} \log P(\mathbf{X}_K, \mathbf{Y}_K|\theta) &= \sum_{t=1}^{T_K} \log P(\mathbf{x}_t|\mathbf{y}_t, \theta_x) + \log P(\mathbf{y}_1|\Sigma_1) \\ &+ \sum_{t=2}^{T_K} \log P(\mathbf{y}_t|\mathbf{y}_{t-1}, \Lambda) \end{aligned} \quad (12)$$

The regularization term is designed as

$$\begin{aligned} \log P(\theta|\mathcal{M}_{i=1}^{K-1}) &\approx -\gamma_{1,K} \|\mathbf{V} - \mathbf{V}_{\mathcal{M}_{K-1}}\|_{\Omega_{\mathcal{M}_{K-1}}^V}^2 \\ &- \gamma_{2,K} \sum_{i=1}^p \Omega_{\mathcal{M}_{K-1},i}^\lambda (\lambda_i - \lambda_{\mathcal{M}_{K-1},i})^2 \end{aligned} \quad (13)$$

where $\Omega_{\mathcal{M}_{K-1}}^V$ and $\Omega_{\mathcal{M}_{K-1},i}^\lambda$ measure the importance of $\mathbf{V}_{\mathcal{M}_{K-1}}$ and $\lambda_{\mathcal{M}_{K-1},i}$, $i = 1, \dots, p$. $\lambda_{\mathcal{M}_{K-1},i}$ and $\Omega_{\mathcal{M}_{K-1},i}^\lambda$ are the i th elements of diagonal matrices $\Lambda_{\mathcal{M}_K}$ and $\Omega_{\mathcal{M}_{K-1}}^\Lambda$, which are the optimal parameters of last mode \mathcal{M}_{K-1} . $\gamma_{1,K}$ and $\gamma_{2,K}$ are user-defined hyperparameters. The setting $\gamma_{1,K}$ and $\gamma_{2,K}$ makes it flexible to adjust the weights of previous modes. Then we illustrate the difference $\gamma_{1,K}$ and $\gamma_{2,K}$ to η_{K-1}^Λ and η_{K-1}^V . Combined with the importance of current mode \mathcal{M}_K , the setting $\gamma_{1,K}$ and $\gamma_{2,K}$ is beneficial to assign the importance of all previous $K-1$ modes again. η_{K-1}^Λ and η_{K-1}^V focus on the importance of the mode \mathcal{M}_{K-1} , which

allow users to obtain models with more focus on particular mode. Through the reasonable setting of four hyperparameters, the human-level performance may be obtained.

For the proposed PSFA-EWC, the total objective function of K modes can be formally described by

$$\begin{aligned} J(\theta) &= \sum_{t=1}^{T_K} \log P(\mathbf{x}_t|\mathbf{y}_t, \theta_x) + \sum_{t=2}^{T_K} \log P(\mathbf{y}_t|\mathbf{y}_{t-1}, \Lambda) \\ &+ \log P(\mathbf{y}_1|\Sigma_1) - \gamma_{1,K} \|\mathbf{V} - \mathbf{V}_{\mathcal{M}_{K-1}}\|_{\Omega_{\mathcal{M}_{K-1}}^V}^2 \\ &- \gamma_{2,K} \sum_{i=1}^p \Omega_{\mathcal{M}_{K-1},i}^\lambda (\lambda_i - \lambda_{\mathcal{M}_{K-1},i})^2 \end{aligned} \quad (14)$$

subject to the PSFA model (1). Note that for $K > 2$, since the quadratic penalty is added, it slows down the changes to parameters with respect to the previously optimum values that are obtained in learned modes [21], [25]. In other words, the parameters that result in significant deterioration in performance of previous modes will be penalized, avoiding catastrophic forgetting problem.

The EM [30] is employed to optimize the parameter $\theta = \{\mathbf{V}, \Lambda, \Sigma_x, \Sigma_1\}$. Note that when $K = 1$, $\Omega_{\mathcal{M}_{K-1}}^V = \mathbf{0}$, $\Omega_{\mathcal{M}_{K-1}}^\Lambda = \mathbf{0}$. There is no need to provide $\mathbf{V}_{\mathcal{M}_{K-1}}$ and $\Lambda_{\mathcal{M}_{K-1}}$, this means that the proposed PSFA-EWC algorithm has a unified formulation as a sequential single mode based on K th mode data only, with current parameters used as quadratic penalty, which are updated via recursive Laplacian approximation between each mode in Section III-A.

EM algorithm for solving (14):

1) **E-step**: Assume that θ is available, the E-step estimates three sufficient statistics, namely, $\mathbb{E}[\mathbf{y}_t|\mathbf{X}_K]$, $\mathbb{E}[\mathbf{y}_t\mathbf{y}_{t-1}|\mathbf{X}_K]$ and $\mathbb{E}[\mathbf{y}_t\mathbf{y}_t^T|\mathbf{X}_K]$. Similar to [11], [13], Kalman filter and Tanch-Tung-Striebel (RTS) smoother [32] are adopted, which contains the forward and backward recursion steps.

First, the forward recursions are adopted to estimate the posterior distribution $P(\mathbf{y}_t|\mathbf{x}_1, \mathbf{x}_2, \dots, \mathbf{x}_t, \theta^{old}) \sim N(\boldsymbol{\mu}_t, \mathbf{U}_t)$ sequentially. The posterior marginal is calculated by

$$\begin{aligned} &\int N(\mathbf{y}_{t-1}|\boldsymbol{\mu}_{t-1}, \mathbf{U}_{t-1}) N(\mathbf{y}_t|\Lambda\mathbf{y}_{t-1}, \Sigma) d\mathbf{y}_{t-1} \\ &= N(\mathbf{y}_t|\Lambda\mathbf{y}_{t-1}, \mathbf{P}_{t-1}) \end{aligned}$$

where \mathbf{P}_{t-1} is the variance.

Then, parameters of the posterior distribution $P(\mathbf{Y}_K|\mathbf{X}_K, \theta^{old})$ are acquired by backward recursion steps. The procedure is summarized in Algorithm 1.

2) **M-step**: In the M-step, it is assumed that three sufficient statistics are fixed, the parameters are updated alternately.

Since \mathbf{V} and Σ_x are contained in $P(\mathbf{x}_t, \mathbf{y}_t|\theta_x)$ and the regularization term $\gamma_{1,K} \|\mathbf{V} - \mathbf{V}_{\mathcal{M}_{K-1}}\|_{\Omega_{\mathcal{M}_{K-1}}^V}^2$, then

$$\{\mathbf{V}^{new}, \Sigma_x^{new}\} = \arg \max_{\mathbf{V}, \Sigma_x} J(\mathbf{V}, \Sigma_x) \quad (15)$$

where

Algorithm 1 E-step in PSFA-EWC

Inputs: $\Sigma_1, \Sigma_x, \Lambda, \mathbf{V}, \mathbf{X}_K$
Outputs: $\mathbb{E}[\mathbf{y}_t|\mathbf{X}_K], \mathbb{E}[\mathbf{y}_t\mathbf{y}_{t-1}^T|\mathbf{X}_K], \mathbb{E}[\mathbf{y}_t\mathbf{y}_t^T|\mathbf{X}_K]$

% Forward steps by Kalman filter:

 1: Initialize $\mathbf{K}_1 = \Sigma_1 \mathbf{V}^T (\mathbf{V} \Sigma_1 \mathbf{V}^T + \Sigma_x)^{-1}$, $\boldsymbol{\mu}_1 = \mathbf{K}_1 \mathbf{x}_1$, $\mathbf{U}_1 = (\mathbf{I} - \mathbf{K}_1 \mathbf{V}) \Sigma_1$

 2: for $t = 1 : T_K$ do

 3: $\mathbf{P}_{t-1} = \Lambda (\mathbf{U}_{t-1} - \mathbf{I}) \Lambda^T + \mathbf{I}$

 4: $\mathbf{K}_t = \mathbf{P}_{t-1} \mathbf{V}^T (\mathbf{V} \mathbf{P}_{t-1} \mathbf{V}^T + \Sigma_x)^{-1}$

 5: $\boldsymbol{\mu}_t = \Lambda \boldsymbol{\mu}_{t-1} + \mathbf{K}_t (\mathbf{x}_t - \mathbf{V} \Lambda \boldsymbol{\mu}_{t-1})$

 6: $\mathbf{U}_t = (\mathbf{I} - \mathbf{K}_t \mathbf{V}) \mathbf{P}_{t-1}$

7: end for

% Backward steps by RTS smoother

 8: Initialize $\hat{\boldsymbol{\mu}}_{T_K} = \boldsymbol{\mu}_{T_K}$, $\hat{\mathbf{U}}_{T_K} = \mathbf{U}_{T_K}$

 9: for $t = T_K : 2$ do

 10: $\mathbf{J}_{t-1} = \mathbf{U}_{t-1} \Lambda^T \mathbf{P}_{t-1}^{-1}$

 11: $\hat{\boldsymbol{\mu}}_{t-1} = \boldsymbol{\mu}_{t-1} + \mathbf{J}_{t-1} (\hat{\boldsymbol{\mu}}_t - \Lambda \boldsymbol{\mu}_{t-1})$

 12: $\hat{\mathbf{U}}_{t-1} = \mathbf{U}_{t-1} + \mathbf{J}_{t-1} (\hat{\mathbf{U}}_t - \mathbf{P}_{t-1}) \mathbf{J}_{t-1}^T$

13: end for

% Calculate the sufficient statistics

 14: for $t = 1 : T_K$ do

 15: $\mathbb{E}[\mathbf{y}_t|\mathbf{X}_K] = \hat{\boldsymbol{\mu}}_t$

 16: $\mathbb{E}[\mathbf{y}_t\mathbf{y}_{t-1}^T|\mathbf{X}_K] = \mathbf{J}_{t-1} \hat{\mathbf{U}}_t + \hat{\boldsymbol{\mu}}_t \hat{\boldsymbol{\mu}}_{t-1}^T$

 17: $\mathbb{E}[\mathbf{y}_t\mathbf{y}_t^T|\mathbf{X}_K] = \hat{\mathbf{U}}_t + \hat{\boldsymbol{\mu}}_t \hat{\boldsymbol{\mu}}_t^T$

 18: end for

$$\begin{aligned}
 & J(\mathbf{V}, \Sigma_x) \\
 &= \sum_{t=1}^{T_K} \log P(\mathbf{x}_t, \mathbf{y}_t | \theta_x) - \gamma_{1,K} \|\mathbf{V} - \mathbf{V}_{\mathcal{M}_{K-1}}\|_{\Omega_{\mathcal{M}_{K-1}}^V}^2 \\
 &= -\frac{T_K}{2} \log |\Sigma_x| - \frac{1}{2} \sum_{t=1}^{T_K} \left(\text{tr}(\mathbb{E}[\mathbf{y}_t \mathbf{y}_t^T | \mathbf{X}_K]) \mathbf{V}^T \Sigma_x^{-1} \mathbf{V} \right. \\
 &\quad \left. + \text{tr}(\mathbf{x}_t \mathbf{x}_t^T \Sigma_x^{-1}) - 2 \text{tr}(\mathbf{x}_t^T \Sigma_x^{-1} \mathbf{V} \mathbb{E}[\mathbf{y}_t | \mathbf{X}_K]) \right) \\
 &\quad - \gamma_{1,K} \text{tr} \left((\mathbf{V} - \mathbf{V}_{\mathcal{M}_{K-1}})^T \Omega_{\mathcal{M}_{K-1}}^V (\mathbf{V} - \mathbf{V}_{\mathcal{M}_{K-1}}) \right)
 \end{aligned}$$

 Let the derivative with respect to \mathbf{V} be zero, then

$$\begin{aligned}
 & \sum_{t=1}^{T_K} \mathbf{x}_t \mathbb{E}[\mathbf{y}_t^T | \mathbf{X}_K] + \gamma_{1,K} \Sigma_x \Omega_{\mathcal{M}_{K-1}}^V \mathbf{V}_{\mathcal{M}_{K-1}} \\
 &= \mathbf{V} \sum_{t=1}^{T_K} \mathbb{E}[\mathbf{y}_t \mathbf{y}_t^T | \mathbf{X}_K] + \gamma_{1,K} \Sigma_x \Omega_{\mathcal{M}_{K-1}}^V \mathbf{V}
 \end{aligned} \tag{16}$$

 This problem is actually the Sylvester equation and the solution is denoted as \mathbf{V}^{new} .

 For $\Sigma_x = \text{diag}(\sigma_1^2, \dots, \sigma_m^2)$, let the derivative be 0, then

$$\begin{aligned}
 (\sigma_i^2)^{new} &= \frac{1}{T_K} \sum_{t=1}^{T_K} \left\{ \mathbb{E}[x_{i,t}^2] - 2(\mathbf{v}_i^T)^{new} \mathbb{E}[\mathbf{y}_t | \mathbf{X}_K] x_{i,t} \right. \\
 &\quad \left. + (\mathbf{v}_i^T)^{new} \mathbb{E}[\mathbf{y}_t \mathbf{y}_t^T | \mathbf{X}_K] (\mathbf{v}_i)^{new} \right\}
 \end{aligned} \tag{17}$$

 where $(\mathbf{v}_i^T)^{new}$ is the i th row of matrix \mathbf{V}^{new} , $1 \leq i \leq m$, and $\Sigma_x^{new} = \text{diag}((\sigma_1^2)^{new}, \dots, (\sigma_m^2)^{new})$.

 With regard to Σ_1 , it is only contained in $P(\mathbf{y}_1)$, thus

$$\begin{aligned}
 \Sigma_1^{new} &= \arg \max_{\Sigma_1} \mathbb{E}[P(\mathbf{y}_1 | \Sigma_1)] \\
 &= \mathbb{E}[\mathbf{y}_1 \mathbf{y}_1^T | \mathbf{X}_K]
 \end{aligned} \tag{18}$$

 For $\Lambda = \text{diag}(\lambda_1, \dots, \lambda_p)$, $\Sigma = \mathbf{I} - \Lambda^2$. λ_i is contained

 in $\Omega_{\mathcal{M}_{K-1},i}^\lambda (\lambda_i - \lambda_{\mathcal{M}_{K-1},i})^2$ and $P(\mathbf{y}_t | \mathbf{y}_{t-1}, \Lambda)$, thus

$$\Lambda^{new} = \arg \max_{\Lambda} J(\Lambda) \tag{19}$$

where

$$\begin{aligned}
 & J(\Lambda) \\
 &= \sum_{t=2}^{T_K} \log P(\mathbf{y}_t | \mathbf{y}_{t-1}, \Lambda) - \gamma_{2,K} \sum_{i=1}^p \Omega_{\mathcal{M}_{K-1},i}^\lambda (\lambda_i - \lambda_{\mathcal{M}_{K-1},i})^2 \\
 &= -\frac{1}{2} \sum_{t=2}^{T_K} \sum_{i=1}^p \left[\log(1 - \lambda_i^2) + \frac{1}{1 - \lambda_i^2} (\mathbb{E}[y_{t,i}^2 | \mathbf{X}_K] \right. \\
 &\quad \left. - 2\lambda_i \mathbb{E}[y_{t,i} y_{t-1,i} | \mathbf{X}_K] + \lambda_i^2 \mathbb{E}[y_{t-1,i}^2 | \mathbf{X}_K]) \right] \\
 &\quad - \gamma_{2,K} \sum_{i=1}^p \Omega_{\mathcal{M}_{K-1},i}^\lambda (\lambda_i - \lambda_{\mathcal{M}_{K-1},i})^2
 \end{aligned}$$

 Let the derivative with respect to λ_i be zero, we drive the following equation

$$a_{i5} \lambda_i^5 + a_{i4} \lambda_i^4 + a_{i3} \lambda_i^3 + a_{i2} \lambda_i^2 + a_{i1} \lambda_i + a_{i0} = 0 \tag{20}$$

where the coefficients of (20) are derived as

$$a_{i5} = 2\gamma_{2,K} \Omega_{\mathcal{M}_{K-1},i}^\lambda,$$

$$a_{i4} = -2\gamma_{2,K} \Omega_{\mathcal{M}_{K-1},i}^\lambda \lambda_{\mathcal{M}_{K-1},i},$$

$$a_{i3} = T_K - 1 - 4\gamma_{2,K} \Omega_{\mathcal{M}_{K-1},i}^\lambda,$$

$$a_{i2} = 4\gamma_{2,K} \Omega_{\mathcal{M}_{K-1},i}^\lambda \lambda_{\mathcal{M}_{K-1},i} - \sum_{t=2}^{T_K} \mathbb{E}[y_{t,i} y_{t-1,i} | \mathbf{X}_K],$$

$$a_{i1} = 2\gamma_{2,K} \Omega_{\mathcal{M}_{K-1},i}^\lambda + \sum_{t=2}^{T_K} (\mathbb{E}[y_{t-1,i}^2 | \mathbf{X}_K] + \mathbb{E}[y_{t,i}^2 | \mathbf{X}_K] - 1),$$

$$a_{i0} = -2\gamma_{2,K} \Omega_{\mathcal{M}_{K-1},i}^\lambda \lambda_{\mathcal{M}_{K-1},i} - \sum_{t=2}^{T_K} \mathbb{E}[y_{t,i} y_{t-1,i} | \mathbf{X}_K]$$

 Thus, the updated λ_i^{new} could be calculated numerically as the root of (20) within the range $[0, 1)$, and $\Lambda^{new} = \text{diag}(\lambda_1^{new}, \dots, \lambda_p^{new})$.

 The learning procedure of PSFA-EWC is summarized in Algorithm 2. The transformation and emission matrices are denoted as $\Lambda_{\mathcal{M}_K}$ and $\mathbf{V}_{\mathcal{M}_K}$, respectively. Since noise information about Σ_1 and Σ_x is only effective for the current mode, the subscript \mathcal{M}_K is neglected. After the mode \mathcal{M}_K has been learned, the parameter importance measures should be updated by (9-10).

IV. MONITORING PROCEDURE AND EXPERIMENT DESIGN

Analogous to traditional PSFA [12], three monitoring statistics are designed to provide a comprehensive operating status. Then, several representative methods are adopted as comparisons to illustrate the superiorities of PSFA-EWC algorithm.

A. Monitoring procedure

 In this paper, the Hotelling's T^2 and SPE statistics are used to reflect the steady variations, and S^2 is calculated to evaluate the temporal dynamics [12].

According to Kalman filter equation,

$$\mathbf{y}_t = \mathbf{\Lambda}_{\mathcal{M}_K} \mathbf{y}_{t-1} + \mathbf{K} [\mathbf{x}_t - \mathbf{V}_{\mathcal{M}_K} \mathbf{\Lambda}_{\mathcal{M}_K} \mathbf{y}_{t-1}] \quad (21)$$

When $t \rightarrow \infty$, \mathbf{K}_t converges to a steady matrix \mathbf{K} . \mathbf{K}_t is stable after the training phase. Then, T^2 statistic is defined as

$$T^2 = \mathbf{y}_t^T \mathbf{y}_t \quad (22)$$

To design the SPE statistic, we calculate the bias between the true value and one-step prediction at t instant. At $t - 1$ instant, the inferred slow features follow Gaussian distribution, namely,

$$P(\mathbf{y}_{t-1} | \mathbf{x}_1, \dots, \mathbf{x}_{t-1}) \sim N(\boldsymbol{\mu}_{t-1}, \mathbf{P}_{t-1})$$

Then, the conditional distribution of \mathbf{y}_t is described as

$$P(\mathbf{y}_t | \mathbf{x}_1, \dots, \mathbf{x}_{t-1}) \sim N(\mathbf{\Lambda}_{\mathcal{M}_K} \boldsymbol{\mu}_{t-1}, \mathbf{\Lambda}_{\mathcal{M}_K} \mathbf{P}_{t-1} \mathbf{\Lambda}_{\mathcal{M}_K}^T + \boldsymbol{\Sigma})$$

Similarly,

$$P(\mathbf{x}_t | \mathbf{x}_1, \dots, \mathbf{x}_{t-1}) \sim N(\mathbf{V}_{\mathcal{M}_K} \mathbf{\Lambda}_{\mathcal{M}_K} \boldsymbol{\mu}_{t-1}, \boldsymbol{\Phi}_t)$$

where $\boldsymbol{\Phi}_t = \mathbf{V}_{\mathcal{M}_K} \mathbf{\Lambda}_{\mathcal{M}_K} \mathbf{P}_{t-1} \mathbf{\Lambda}_{\mathcal{M}_K}^T \mathbf{V}_{\mathcal{M}_K}^T + \mathbf{V}_{\mathcal{M}_K} \boldsymbol{\Sigma} \mathbf{V}_{\mathcal{M}_K}^T + \boldsymbol{\Sigma}_x$. The prediction error follows Gaussian distribution, namely

$$\boldsymbol{\varepsilon}_t = \mathbf{x}_t - \mathbf{V}_{\mathcal{M}_K} \mathbf{\Lambda}_{\mathcal{M}_K} \boldsymbol{\mu}_{t-1} \sim N(\mathbf{0}, \boldsymbol{\Phi}_t) \quad (23)$$

When $t \rightarrow \infty$, $\boldsymbol{\Phi}_t$ converges to $\boldsymbol{\Phi}$. SPE is calculated by

$$\text{SPE} = \boldsymbol{\varepsilon}_t^T \boldsymbol{\Phi}^{-1} \boldsymbol{\varepsilon}_t \quad (24)$$

S^2 statistic is designed to reflect the temporal dynamics, which is beneficial to distinguish the operating variations and dynamics anomalies [8], [12].

$$S^2 = \dot{\mathbf{y}}_t^T \boldsymbol{\Xi}^{-1} \dot{\mathbf{y}}_t \quad (25)$$

where $\dot{\mathbf{y}}_t = \mathbf{y}_t - \mathbf{y}_{t-1}$, $\boldsymbol{\Xi} = \mathbb{E}\{\dot{\mathbf{y}}_t \dot{\mathbf{y}}_t^T\}$ is the covariance matrix and analytically calculated as $\boldsymbol{\Xi} = 2(\mathbf{I}_p - \mathbf{\Lambda}_{\mathcal{M}_K})$ [12].

The thresholds of three statistics are calculated by kernel density estimation (KDE) [1], and denoted as J_{th, T^2} , $J_{th, \text{SPE}}$ and J_{th, S^2} . The monitoring rule is summarized below:

- 1) Three statistics are within their thresholds, the process is

Algorithm 2 Off-line training procedure of PSFA-EWC

Inputs: $\tilde{\mathbf{X}}_K, p, \mathbf{V}_{\mathcal{M}_{K-1}}, \mathbf{\Lambda}_{\mathcal{M}_{K-1}}, \boldsymbol{\Omega}_{\mathcal{M}_{K-1}}^V, \boldsymbol{\Omega}_{\mathcal{M}_{K-1}}^\Lambda$

Outputs: $\boldsymbol{\mu}_K, \boldsymbol{\Sigma}_K, \mathbf{V}_{\mathcal{M}_K}, \mathbf{\Lambda}_{\mathcal{M}_K}, \boldsymbol{\Omega}_{\mathcal{M}_K}^V, \boldsymbol{\Omega}_{\mathcal{M}_K}^\Lambda, \mathbf{K}, \boldsymbol{\Phi}, \boldsymbol{\Xi}, J_{th, T^2}, J_{th, \text{SPE}}$ and J_{th, S^2}

- 1: For the mode \mathcal{M}_K , collect normal data $\tilde{\mathbf{X}}_K$, calculate the mean $\boldsymbol{\mu}_K$ and standard variance $\boldsymbol{\Sigma}_K$. Normalize data and the scaled data are denoted as \mathbf{X}_K ;
 - 2: Initialize parameters $\mathbf{V}, \mathbf{\Lambda}, \boldsymbol{\Sigma}_1, \boldsymbol{\Sigma}_x, \boldsymbol{\Sigma}$;
 - 3: **While** the issue (14) is not converged **do**
 - a) Calculate three sufficient statistics based on Algorithm 1;
 - b) Update the parameters by (16, 17, 18, 20);
 - 4: The optimal emission and transition matrices are denoted as $\mathbf{V}_{\mathcal{M}_K}$ and $\mathbf{\Lambda}_{\mathcal{M}_K}$, respectively;
 - 5: Calculate the FIMs $\mathbf{F}_{\mathcal{M}_K}^V$ by (28) and $\mathbf{F}_{\mathcal{M}_K}^\Lambda$ by (30). Then, update the importance measures $\boldsymbol{\Omega}_{\mathcal{M}_K}^V$ and $\boldsymbol{\Omega}_{\mathcal{M}_K}^\Lambda$ by (9-10);
 - 6: The final Kalman matrix is denoted as \mathbf{K} , calculate $\boldsymbol{\Phi}$ and $\boldsymbol{\Xi}$;
 - 7: Calculate three monitoring statistics by (22, 24, 25);
 - 8: Calculate thresholds by KDE, labeled as $J_{th, T^2}, J_{th, \text{SPE}}$ and J_{th, S^2} .
-

TABLE I
COMPARATIVE SCHEMES

	Methods	Training sources (Model + Data)	Model label	Testing sources
Situation 1	PSFA	\mathcal{M}_1	A	\mathcal{M}_1
Situation 2	PSFA-EWC	A + \mathcal{M}_2	B	\mathcal{M}_2
Situation 3	PSFA-EWC	-	B	\mathcal{M}_1
Situation 4	PSFA	\mathcal{M}_2	C	\mathcal{M}_2
Situation 5	PSFA	-	C	\mathcal{M}_1
Situation 6	PSFA-EWC	B + \mathcal{M}_3	D	\mathcal{M}_3
Situation 7	PSFA-EWC	-	D	\mathcal{M}_1
Situation 8	PSFA-EWC	-	D	\mathcal{M}_2
Situation 9	PSFA	\mathcal{M}_3	E	\mathcal{M}_3
Situation 10	PSFA	-	E	\mathcal{M}_1
Situation 11	PSFA	-	E	\mathcal{M}_2
Situation 12	RSFA	\mathcal{M}_1	F	\mathcal{M}_1
Situation 13	RSFA	F + \mathcal{M}_2	G	\mathcal{M}_2
Situation 14	RSFA	G + \mathcal{M}_3	H	\mathcal{M}_3
Situation 15	PCA	\mathcal{M}_1	I	\mathcal{M}_1
Situation 16	PCA-EWC	I + \mathcal{M}_2	J	\mathcal{M}_2
Situation 17	PCA-EWC	-	J	\mathcal{M}_1
Situation 18	PCA-EWC	J + \mathcal{M}_3	L	\mathcal{M}_3
Situation 19	PCA-EWC	-	L	\mathcal{M}_1
Situation 20	PCA-EWC	-	L	\mathcal{M}_2
Situation 21	IMPPCA	$\mathcal{M}_1, \mathcal{M}_2$	M	\mathcal{M}_1
Situation 22	IMPPCA	-	M	\mathcal{M}_2
Situation 23	IMPPCA	$\mathcal{M}_1, \mathcal{M}_2, \mathcal{M}_3$	N	\mathcal{M}_1
Situation 24	IMPPCA	-	N	\mathcal{M}_2
Situation 25	IMPPCA	-	N	\mathcal{M}_3
Situation 26	MCVA	$\mathcal{M}_1, \mathcal{M}_2$	O	\mathcal{M}_1
Situation 27	MCVA	-	O	\mathcal{M}_2
Situation 28	MCVA	$\mathcal{M}_1, \mathcal{M}_2, \mathcal{M}_3$	P	\mathcal{M}_1
Situation 29	MCVA	-	P	\mathcal{M}_2
Situation 30	MCVA	-	P	\mathcal{M}_3

normal;

- 2) If T^2 or SPE is over its threshold, while S^2 is below its threshold, the dynamic law remains unchanged and the static variations occur. This may be caused by step faults or drifts may occur [8], [10]. In this case, we need to further confirm whether the system is actually abnormal based on the data trend and expert experience. When a new mode occurs, a set of new data are collected to update the PSFA-EWC model in Algorithm 2. The process is monitored by S^2 statistic in this period;
- 3) If S^2 is over threshold, the dynamic behaviors are unusual and the system is out of control. A fault occurs and the alarm would be triggered.

The off-line training procedure and online monitoring phase have been summarized in Algorithm 2 and Algorithm 3, respectively. Fault detection rates (FDRs) and false alarm rates (FARs) are adopted to evaluate the performance.

Algorithm 3 Online monitoring of PSFA-EWC

- 1: Collect the test data \mathbf{x} , preprocess \mathbf{x} by $\boldsymbol{\mu}_K$ and $\boldsymbol{\Sigma}_K$;
 - 2: Calculate the latent variable by (21) and prediction error by (23);
 - 3: Calculate three monitoring statistics by (22, 24, 25);
 - 4: Judge the operating condition:
 - a) Normal, return to step 1;
 - b) A new mode appears, let $K = K + 1$, return to Algorithm 2 to update the monitoring model;
 - c) A fault occurs and the alarm is triggered.
-

B. Comparative design

In this paper, RSFA [9], PCA-EWC [27], IMPPCA [1] and MCVA [18] are selected as the comparative methods in Table I. PSFA-EWC, RSFA and PCA-EWC can be regarded as adaptive methods, which avoid storing data and alleviating storage requirement. IMPPCA and MCVA belong to multiple-model approaches, where the mode is identified and local models are built within each mode.

For Situations 1-11, PSFA and PSFA-EWC are compared to illustrate the catastrophic forgetting issue of PSFA and the continual learning ability of PSFA-EWC for successive dynamic modes. When a new mode is identified by S^2 statistic and expert experience, a set of normal data are collected and then the model is updated off-line by consolidating new information while retaining the learned knowledge. PSFA-EWC furnishes the backward and forward transfer ability. The updated model is able to monitor the previous modes and the learned knowledge is valuable to learn new relevant modes. Equivalently, the simulation results of Situations 2, 3, 6-8 should be excellent. Conversely, the consequences of Situations 5, 10 and 11 are expected to be poor, thus the catastrophic forgetting issue is reflected. The RSFA monitoring model is updated in real time and expected to track the system adaptively, as Situations 12-14 illustrated. For Situations 15-20, the design process of PCA-EWC is similar to that of PSFA-EWC. PCA-EWC is desired to provide the continual learning ability comparable to PSFA-EWC.

For IMPPCA and MCVA, data from all possible modes are required and stored before learning. When a novel mode arrives, sufficient samples should be collected and the model needs to be retrained on the entire dataset. For example, when mode \mathcal{M}_3 appears, the model is relearned based on data from three modes. The model can deliver optimal monitoring consequences for the learned modes. Intuitively, IMPPCA and MCVA should provide the outstanding performance for Situations 21-30. However, it is intractable and time-consuming to collect all mode data in practical systems [14]. Besides, the computational resources would increase for each retraining with the increasing number of modes.

V. CASE STUDIES

A. CSTH case

The CSTH process is a nonlinear dynamic process and widely utilized as a benchmark for multimode process monitoring [19], [33]. Thornhill *et al.* built the CSTH model and the detail information was described in [34]. CSTH aims to mix the hot and cold water with desirable settings. Level, temperature and flow are manipulated by PI controllers. Six critical variables are selected for monitoring in this paper.

This paper designs two cases and three successive modes are considered in each case, as listed in Table II. For each mode, 1000 normal samples are collected and 1000 testing samples are generated as follows:

- Case 1: a random fault occurs in the level from 501th sample and the fault amplitude is 0.15;
- Case 2: a random fault occurs in the temperature from 501th sample and the fault amplitude is 0.18.

For PSFA-EWC, PSFA and RSFA, the evaluation indices of three monitoring statistics are summarized in Table III. S^2 statistic is established to reflect the dynamic behaviors and the occurrence of a fault is confirmed for multimode processes. Three comparative methods calculate two statistics and a fault is detected when SPE or T^2 is beyond the corresponding threshold. The simulation results of PCA-EWC, IMPPCA and MCVA are concluded in Table IV.

For Case 1, PSFA-EWC provides excellent performance for successive modes and the unusual dynamic behaviors can be detected by S^2 statistic. In particular, the detection accuracy of Situations 2 and 3 is generally higher than that of Situations 1, 4 and 5. For Situation 2-3, the FDRs of S^2 approach 100% while the FDRs are less than 90% for other three situations. The FDRs of T^2 or SPE are similar for these five situations. Similarly, for Situations 6-11, the FDRs of SPE statistic are basically at 92% ~ 94%. However, for Situation 6-8, the FDRs of S^2 are higher than those of Situations 9-11. Compared with PSFA, the previously learned knowledge is preserved while sequential modes are trained, which is sufficient to deliver outstanding performance for previous modes. Besides, PSFA-EWC can transfer knowledge between modes. For instance, the monitoring results of Situation 2 are superior to Situation 4. S^2 is an important index to detect the abnormality from dynamic features in multimode processes, which indicates that PSFA-EWC is preferred because the FDRs of S^2 are satisfactory. The previously learned knowledge contributes to building an accurate model for future relevant modes, thus the forward transfer ability is reflected. For Situations 12-14, RSFA fails to monitor the successive modes based on an adaptive model, where the FDRs of S^2 are less than 65%. RSFA is difficult to track the dramatic variations on the entire dataset. Analogous to PSFA-EWC, PCA-EWC is expected to offer prominent performance for sequential modes. However, the FDRs of Situations 16-20 cannot compare with the corresponding situations of PSFA-EWC. Although both methods utilize EWC to preserve the previously learned knowledge, PSFA can deal with dynamic slow features and S^2 is designed to reflect the unusual dynamic behaviors, while PCA is suitable to static data in each mode. IMPPCA and MCVA build the local models in each mode and the model needs to be retrained on the entire dataset when a new mode arrives. They deliver outstanding monitoring consequences for the learned modes, especially for MCVA.

Similar to Case 1, the monitoring results of Case 2 are analyzed succinctly. PSFA-EWC and PSFA offer the similar FDRs of T^2 or SPE, but PSFA-EWC has higher FDRs of S^2

TABLE II
NORMAL OPERATING MODES OF CSTH

Case number	Mode	Level SP	Temperature SP	Hot water valve
Case 1	\mathcal{M}_1	9	10.5	4.5
	\mathcal{M}_2	12	8	4
	\mathcal{M}_3	12	10.5	5.5
Case 2	\mathcal{M}_1	13	10.5	5
	\mathcal{M}_2	11	10.5	4.5
	\mathcal{M}_3	12	10.5	5

TABLE III
FDRs (%) AND FARs (%) FOR PSFA, PSFA-EWC AND RSFA

Fault type	Method	Case 1						Case 2						Case 3					
		T^2		SPE		S^2		T^2		SPE		S^2		T^2		SPE		S^2	
		FDR	FAR	FDR	FAR	FDR	FAR	FDR	FAR	FDR	FAR	FDR	FAR	FDR	FAR	FDR	FAR	FDR	FAR
Situation 1	PSFA	27.0	2.2	92.8	0.2	80.2	0.6	8.0	2.2	91.8	2.2	79.4	3.8	99.89	0.36	97.20	0	53.03	2.74
Situation 2	PSFA-EWC	90.0	0	79.0	0	98.6	1.0	12.6	0	91.6	4.4	77.4	6.0	99.27	0	99.45	0	60.40	1.69
Situation 3	PSFA-EWC	91.2	0	81.2	0	99.0	8.8	18.6	4.2	91.8	2.8	78.6	5.6	99.89	0	99.89	0	66.37	8.39
Situation 4	PSFA	0	0	92.2	0.2	77.0	0.4	16.2	0.4	90.2	2.8	71.0	4.8	99.45	4.70	99.45	0	63.87	1.69
Situation 5	PSFA	0	0	92.8	1.2	86.0	15.0	18.8	5.6	91.2	5.2	74.2	4.8	99.89	3.83	99.89	11.31	92.83	21.17
Situation 6	PSFA-EWC	11.6	4.0	93.2	0	60.6	1.0	8.0	2.0	94.0	3.6	74.8	6.4	100	0.16	99.58	0.32	95.40	4.80
Situation 7	PSFA-EWC	12.8	0	93.0	0.6	67.0	0.4	10.0	2.6	92.2	3.8	78.4	6.6	99.89	0	99.89	0	94.51	16.06
Situation 8	PSFA-EWC	7.4	11.8	92.6	0	64.0	1.4	6.4	0	92.4	5.4	77.4	8.2	98.91	0	99.45	0	81.02	2.82
Situation 9	PSFA	0	0.6	93.6	0.4	1.0	0	0	1.4	93.6	2.4	8.8	5.2	100	0.32	100	0.16	99.58	4.32
Situation 10	PSFA	0	0	93.6	0.8	3.2	0.2	0	2.4	91.6	2.6	9.0	5.4	99.89	12.96	99.89	0.91	98.54	23.54
Situation 11	PSFA	0	2.2	93.0	1.8	3.2	1.0	0	0	92.0	4.0	13.8	6.8	100	33.27	99.45	11.84	91.24	2.44
Situation 12	RSFA	0	0	0	0	44.2	0.6	0	0	0	0	40.8	1.6	37.00	0	44.39	0	50.56	2.19
Situation 13	RSFA	0	0	0	0	61.4	0.8	0	0	0	0	33.4	0.6	96.48	4.0	0	0	29.23	12.48
Situation 14	RSFA	0	0	0	0	29.6	0.8	0	0	0	0	10.6	0.4	0	0	0	0	12.97	1.44

TABLE IV
FDRs (%) AND FARs (%) FOR PCA-EWC, IMPPCA AND MCVA

Fault type	Method	Case 1				Case 2				Case 3			
		T^2		SPE		T^2		SPE		T^2		SPE	
		FDR	FAR	FDR	FAR	FDR	FAR	FDR	FAR	FDR	FAR	FDR	FAR
Situation 15	PCA	60.2	2.2	92.6	3.4	21.2	2.0	80.6	3.6	99.89	1.46	99.89	0
Situation 16	PCA-EWC	0.4	0	75.4	0.2	11.0	0.4	80.0	1.0	52.19	0	99.45	0
Situation 17	PCA-EWC	0	0	82.8	1.6	11.4	0.6	82.4	4.4	27.58	0	99.89	0
Situation 18	PCA-EWC	12.0	0.6	86.8	4.4	10.6	0.4	79.6	2.4	98.74	0.96	100	0.32
Situation 19	PCA-EWC	13.2	1.0	86.4	0	11.4	0.6	79.2	3.4	54.26	0	99.89	0
Situation 20	PCA-EWC	13.4	1.0	85.4	21.0	11.0	0.6	77.2	0	80.47	0	99.45	0
Situation 21	IMPPCA	91.4	0	19.0	0	51.0	0.8	37.2	2.8	99.89	15.51	99.89	6.39
Situation 22	IMPPCA	3.2	0	92.8	0.4	50.6	0.8	30.6	0	99.45	5.08	99.45	0
Situation 23	IMPPCA	14.2	0	90.4	0	45.4	0.8	0.4	0	99.89	0.73	99.89	0
Situation 24	IMPPCA	4.8	0	92.4	0.2	33.8	0.6	90.6	1.2	99.45	0	99.45	0
Situation 25	IMPPCA	24.8	0.2	93.4	0	42.6	0.8	0.2	0	100	2.24	95.82	0
Situation 26	MCVA	99.8	0.4	91.75	4.8	90.16	5.0	3.41	5.2	100	2.37	96.40	0
Situation 27	MCVA	99.8	0.8	12.68	0	65.26	2.4	2.01	4.2	100	3.83	100	8.39
Situation 28	MCVA	99.8	2.4	88.93	1.4	57.03	3.4	0	0	100	9.85	98.87	0
Situation 29	MCVA	99.8	0.6	24.14	0.6	66.67	3.4	6.83	10.2	100	6.39	99.63	9.77
Situation 30	MCVA	100	3.2	93.36	7.8	55.02	2.0	0	0.2	100	0.48	86.81	0

TABLE V
FAULT INFORMATION AND EXPERIMENTAL DATA OF THE PRACTICAL COAL PULVERIZING SYSTEM

Case number	Key variables	Mode number	NoTrS	NoTeS	Fault location	Fault cause
Case 3	9 variables: pressure of air powder mixture, outlet temperature, primary air pressure and temperature, etc.	\mathcal{M}_1	2520	1440	549	Pulverizer deflagration
		\mathcal{M}_2	1080	1080	533	Hot primary air electric damper failure
		\mathcal{M}_3	1440	864	626	Air leakage at primary air interface

than PSFA, especially for Situations 6-11. For Situations 6-8, the FDRs of S^2 are higher than 70%, while FDRs of Situations 9-11 are lower than 20%. The FDRs of S^2 are 74.8% and 8.8% for Situations 6 and 9, which reveals that the learned knowledge from previous modes contributes to improving the detection rates of mode \mathcal{M}_3 . Briefly, PSFA-EWC furnishes the backward and forward transfer ability. For RSFA, the FDRs of S^2 are less than 41% and partial faulty samples are mistaken for normal data. For Situations 15-20, the FDRs of SPE are lower than 81%, while the FDRs of PSFA-EWC are higher than 90%. The performance of IMPPCA and MCVA are not satisfactory and the FDRs are lower than 70% except for

Situations 24 and 26. Partial monitoring charts are depicted in Fig. 2 owing to space limitation.

Generally speaking, PSFA-EWC outperforms others for sequential modes, where the number of modes and samples per mode are not required in advance. It provides forward and backward transfer ability. The previously learned knowledge is preserved when assimilating new information, which also aids the learning of future relevant modes. The RSFA model is updated when a new sample arrives, but fails to distinguish the normal changes and the real faults in multimode dynamic processes. Compared with PSFA-EWC, PCA-EWC is effective to detect the abnormality from static features but difficult to

identify a new mode. PSFA-EWC, RSFA and PCA-EWC have the basically fixed model capacity, where a single model is updated continually. IMPPCA and MCVA identify the modes and build the local models within each mode. When a new mode arrives, the monitoring model is rebuilt based on the entire dataset and the model complexity would increase with the emergence of novel modes.

B. The pulverizing system

We focus on the coal pulverizing system of the 1000-MW ultra-supercritical thermal power plant in China [27]. The structure is depicted in Fig. 3. The coal pulverizing system grinds the raw coal into pulverized coal with desired fineness and optimal temperature. High temperature may lead to deflagration and low temperature would reduce the combustion efficiency. According to the historical recording, the fault in outlet temperature occurs frequently and thus it is essential to investigate this sort of fault. Data from three successive modes are selected to illustrate the effectiveness, as listed in Table V. The variables are selected by expert experience and prior knowledge. For convenience, the numbers of training and testing samples are denoted as NoTrS and NoTeS, respectively.

The simulation consequences of 30 situations are summarized in Table III and Table IV. PSFA-EWC performs better than PSFA and the significant information preserved in the model is valuable to enhance detection accuracy. The FDRs of Situation 3 are better than those of Situation 1, which indicates that the learned knowledge of mode \mathcal{M}_2 is conducive to monitor mode \mathcal{M}_1 . The FARs of Situations 5,10 and 11 are higher than 20%, which are not acceptable. PSFA suffers from catastrophic forgetting issue, where the model built for one mode may not provide excellent performance for another mode. RSFA cannot monitor the multiple modes accurately and the FDRs of S^2 are lower than 51%. Only the FDR of T^2 is 96.48% for Situation 13. PCA-EWC can detect the faults in successive modes timely and the FDRs approach 100%. IMPPCA and MCVA offer favorable monitoring performance and the FDRs are convincing, except for Situation 21. Partial monitoring results are depicted in Fig. 4.

In conclusion, PSFA-EWC is capable of monitoring the sequential modes accurately and the fault is confirmed by S^2 statistic. The model is updated continually by consolidating new information while preserving the learned knowledge, thus avoiding the performance degradation for similar modes as before. RSFA is effective for dealing with slowly time-varying data and thus fails to track the dramatic changes on the entire dataset. Similar to PSFA-EWC, PCA-EWC enables to monitor the multiple modes based on a updated model for this case. IMPPCA and MCVA are capable of monitoring the learned modes. However, they require the number of modes is a prior before learning and local models are retrained when new modes arrive. In terms of detection accuracy, the model complexity and applications, PSFA-EWC is the most desirable among five typical methods.

VI. CONCLUSION

This paper has introduced a novel extension of elastic weight consolidation to multimode dynamic process monitor-

ing, based on multimode PSFA. The proposed PSFA-EWC method has powerful probabilistic interpretability and ability to deal with the measurement noise. When a new mode arrives, assume that a set of data are collected, the single model is updated by consolidating new information while preserving the learned features. The previously learned knowledge is retained and may be beneficial to establish an accurate model for future relevant modes, thus delivering backward and forward transfer learning ability. The PSFA features are extracted to form meaningful statistics for fault detection covering multimodes with only using recent mode data, with low storage and computational costs. Compared with several state-of-the-art methods, the effectiveness of PSFA-EWC is illustrated by a CSTD case and a practical coal pulverizing system.

In future work, we would investigate the multimode dynamic modes with applications to chemical systems, industrial manufacturing systems, etc. Besides, the modes are diverse and the long-term continual learning ability is desired.

APPENDIX

A. Estimation of Fisher information matrix with PSFA

In order to approximate the posterior probability $P(\theta|\mathcal{M}_{i=1}^{K-1})$, sequentially with incoming modes $K = 2, \dots$, Laplacian approximation [24], [35] is employed, i.e. local Gaussian probability density is used for its approximation centered at maximum posterior probability $\theta_{\mathcal{M}_{K-1}}^*$, with covariance of the gradient of the model's log likelihood function with respect to $\theta_{\mathcal{M}_{K-1}}^*$. The Fisher information matrix is the covariance of the gradient of the model's log likelihood function with respect to the local optimum, which is approximated by

$$\begin{aligned} \mathbf{F} &= \mathbb{E}_{P_{\mathbf{x}, \mathbf{y}}} \left[\nabla \log P(\mathbf{x}, \mathbf{y}|\theta) \nabla \log P(\mathbf{x}, \mathbf{y}|\theta)^T \right] \\ &= \frac{1}{T} \sum_t \left[\nabla \log P(\mathbf{x}_t, \mathbf{y}_t|\theta) \nabla \log P(\mathbf{x}_t, \mathbf{y}_t|\theta)^T \right] \end{aligned} \quad (26)$$

where $\theta = \theta_{\mathcal{M}_{K-1}}^*$ after the mode \mathcal{M}_{K-1} has been learned. The conditional probability is calculated by

$$P(\mathbf{x}_t, \mathbf{y}_t|\theta) = P(\mathbf{x}_t|\mathbf{y}_t, \theta_x) P(\mathbf{y}_t|\theta_y)$$

Within the context of our PSFA model (1), only parameters \mathbf{V} and $\mathbf{\Lambda}$ are considered to calculate the corresponding FIMs, since the Laplacian is based on well-behaved function approximation which may not be applicable to noise. Besides, it is reasonable to assume that variance of unknown noise is constant in our problem.

The gradient with regard to \mathbf{V} is

$$\begin{aligned} \nabla_{\mathbf{V}} \log P(\mathbf{x}_t, \mathbf{y}_t|\theta) &= \frac{\partial \log P(\mathbf{x}_t|\mathbf{y}_t, \theta_x)}{\partial \mathbf{V}} \\ &= \mathbf{\Sigma}_x^{-1} (\mathbf{V} \mathbf{y}_t - \mathbf{x}_t) \mathbf{y}_t^T \end{aligned} \quad (27)$$

When the mode \mathcal{M}_K has been learned, the FIM about \mathbf{V} is computed by

$$\begin{aligned} \mathbf{F}_{\mathcal{M}_K}^{\mathbf{V}} &= \frac{1}{T_K} \sum_t \mathbf{\Sigma}_x^{-1} (\mathbf{V}_{\mathcal{M}_K} \mathbf{y}_t - \mathbf{x}_t) \mathbf{y}_t^T \mathbf{y}_t (\mathbf{V}_{\mathcal{M}_K} \mathbf{y}_t - \mathbf{x}_t)^T \mathbf{\Sigma}_x^{-1} \end{aligned} \quad (28)$$

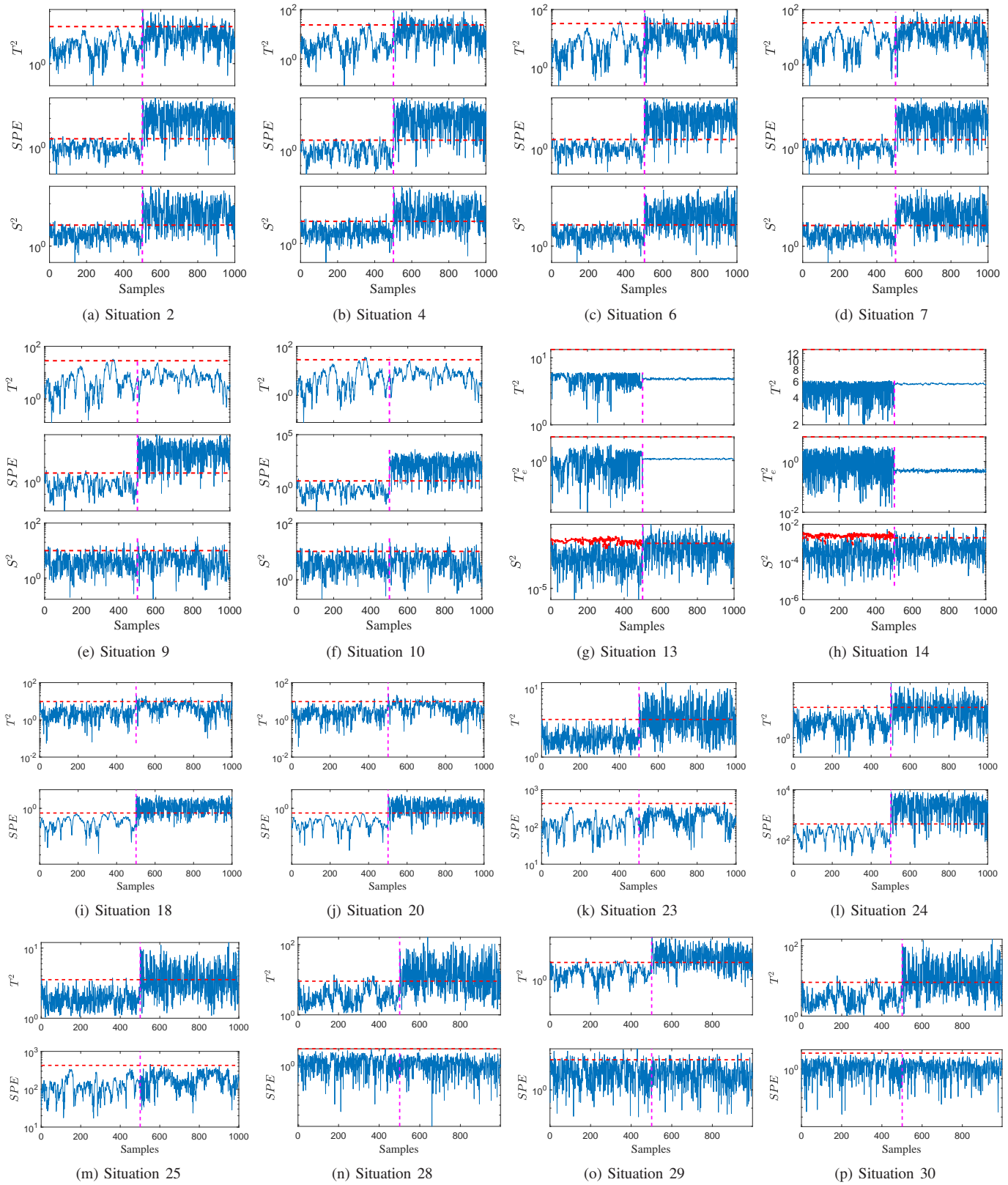


Fig. 2. Monitoring charts of Case 2

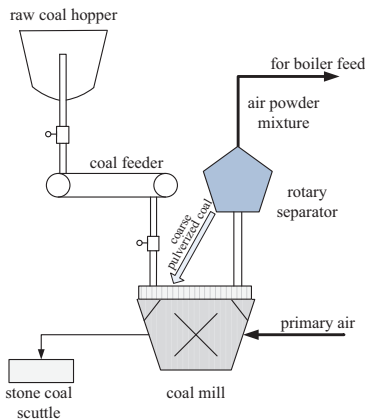


Fig. 3. Schematic diagram of the coal pulverizing system

Since $\Sigma = \mathbf{I} - \Lambda^2$, $\mathbf{y}_t \sim N(\Lambda \mathbf{y}_{t-1}, \Sigma)$, and $\Lambda = \text{diag}(\lambda_1, \dots, \lambda_p)$, the gradient with respect to λ_i is

$$\begin{aligned} & \nabla_{\lambda_i} \log P(\mathbf{x}_t, \mathbf{y}_t | \theta) \\ &= \frac{\partial \log P(\mathbf{y}_t | \theta_y)}{\partial \lambda_i} \\ &= \frac{-\lambda_i^3 + y_{t,i} y_{t-1,i} \lambda_i^2 + (1 - y_{t,i}^2 - y_{t-1,i}^2) \lambda_i + y_{t,i} y_{t-1,i}}{(1 - \lambda_i^2)^2} \\ &\triangleq g(y_{t,i}, y_{t-1,i}, \lambda_i) \end{aligned} \quad (29)$$

For mode \mathcal{M}_K , the FIM about λ_i is

$$F_{\lambda_i} = \frac{1}{T_K} \sum_t g(y_{t,i}, y_{t-1,i}, \lambda_{\mathcal{M}_K, i})^2, i = 1, \dots, p \quad (30)$$

where $\lambda_{\mathcal{M}_K, i}$ is the i th element of diagonal matrix $\Lambda_{\mathcal{M}_K}$, $\mathbf{F}_{\mathcal{M}_K}^\Lambda = \text{diag}(F_{\lambda_1}, \dots, F_{\lambda_p})$.

REFERENCES

- [1] J. Zhang, H. Chen, S. Chen, and X. Hong, "An improved mixture of probabilistic PCA for nonlinear data-driven process monitoring," *IEEE Transactions on Cybernetics*, vol. 49, no. 1, pp. 198–210, 2019.
- [2] J. Yu and X. Yan, "Whole process monitoring based on unstable neuron output information in hidden layers of deep belief network," *IEEE Transactions on Systems, Man, and Cybernetics*, vol. 50, no. 9, pp. 3998–4007, 2020.
- [3] J. Shi, J. Sun, Y. Yang, and D. Zhou, "Distributed self-triggered formation control for multi-agent systems," *Science in China Series F: Information Sciences*, vol. 63, no. 10, pp. 1–3, 2020.
- [4] S. Yin, X. Xie, J. Lam, K. C. Cheung, and H. Gao, "An improved incremental learning approach for KPI prognosis of dynamic fuel cell system," *IEEE Transactions on Systems, Man, and Cybernetics*, vol. 46, no. 12, pp. 3135–3144, 2016.
- [5] S. J. Qin, Y. Dong, Q. Zhu, J. Wang, and Q. Liu, "Bridging systems theory and data science: A unifying review of dynamic latent variable analytics and process monitoring," *Annual Reviews in Control*, vol. 50, pp. 29–48, 2020.
- [6] Y. Jiang and S. Yin, "Recursive total principle component regression based fault detection and its application to vehicular cyber-physical systems," *IEEE Transactions on Industrial Informatics*, vol. 14, no. 4, pp. 1415–1423, 2018.
- [7] L. Wiskott and T. J. Sejnowski, "Slow feature analysis: unsupervised learning of invariances," *Neural Computation*, vol. 14, no. 4, pp. 715–770, 2002.
- [8] C. Shang, F. Yang, X. Gao, X. Huang, J. A. Suykens, and D. Huang, "Concurrent monitoring of operating condition deviations and process dynamics anomalies with slow feature analysis," *AIChE Journal*, vol. 61, no. 11, pp. 3666–3682, 2015.
- [9] C. Shang, F. Yang, B. Huang, and D. Huang, "Recursive slow feature analysis for adaptive monitoring of industrial processes," *IEEE Transactions on Industrial Electronics*, vol. 65, no. 11, pp. 8895–8905, 2018.
- [10] W. Yu and C. Zhao, "Recursive exponential slow feature analysis for fine-scale adaptive processes monitoring with comprehensive operation status identification," *IEEE Transactions on Industrial Informatics*, vol. 15, no. 6, pp. 3311–3323, 2019.
- [11] C. Shang, B. Huang, F. Yang, and D. Huang, "Probabilistic slow feature analysis-based representation learning from massive process data for soft sensor modeling," *AIChE Journal*, vol. 61, no. 12, pp. 4126–4139, 2015.
- [12] F. Guo, C. Shang, B. Huang, K. Wang, F. Yang, and D. Huang, "Monitoring of operating point and process dynamics via probabilistic slow feature analysis," *Chemometrics and Intelligent Laboratory Systems*, vol. 151, no. 151, pp. 115–125, 2016.
- [13] L. Zafeiriou, M. A. Nicolaou, S. Zafeiriou, S. Nikitidis, and M. Pantic, "Probabilistic slow features for behavior analysis," *IEEE Transactions on Neural Networks and Learning Systems*, vol. 27, no. 5, pp. 1034–1048, 2016.
- [14] M. Quiñones-Grueiro, A. Prieto-Moreno, C. Verde, and O. Llanes-Santiago, "Data-driven monitoring of multimode continuous processes: A review," *Chemometrics and Intelligent Laboratory Systems*, vol. 189, pp. 56–71, 2019.
- [15] H. Ma, Y. Hu, and H. Shi, "A novel local neighborhood standardization strategy and its application in fault detection of multimode processes," *Chemometrics and Intelligent Laboratory Systems*, vol. 118, pp. 287–300, 2012.
- [16] H. Wu and J. Zhao, "Self-adaptive deep learning for multimode process monitoring," *Computers & Chemical Engineering*, vol. 141, p. 107024, 2020.
- [17] L. M. Elshenawy, S. Yin, A. S. Naik, and S. X. Ding, "Efficient recursive principal component analysis algorithms for process monitoring," *Industrial & Engineering Chemistry Research*, vol. 49, no. 1, pp. 252–259, 2010.
- [18] Q. Wen, Z. Ge, and Z. Song, "Multimode dynamic process monitoring based on mixture canonical variate analysis model," *Industrial & Engineering Chemistry Research*, vol. 54, no. 5, pp. 1605–1614, 2015.
- [19] K. Huang, Y. Wu, C. Yang, G. Peng, and W. Shen, "Structure dictionary learning-based multimode process monitoring and its application to aluminum electrolysis process," *IEEE Transactions on Automation Science and Engineering*, vol. 17, no. 4, pp. 1989–2003, 2020.
- [20] J. Kirkpatrick, R. Pascanu, N. Rabinowitz, J. Veness, G. Desjardins, A. A. Rusu, K. Milan, J. Quan, T. Ramalho, and A. Grabska-Barwinska, "Overcoming catastrophic forgetting in neural networks," *Proceedings of the National Academy of Sciences of the United States of America*, vol. 114, no. 13, pp. 3521–3526, 2017.
- [21] G. M. van de Ven, H. T. Siegelmann, and A. S. Tolia, "Brain-inspired replay for continual learning with artificial neural networks," *Nature Communications*, vol. 11, no. 1, pp. 4069–4069, 2020.
- [22] R. Hadsell, D. Rao, A. A. Rusu, and R. Pascanu, "Embracing change: Continual learning in deep neural networks," *Trends in Cognitive Sciences*, vol. 24, no. 12, pp. 1028 – 1040, 2020.
- [23] N. Y. Masse, G. D. Grant, and D. J. Freedman, "Alleviating catastrophic forgetting using context-dependent gating and synaptic stabilization," *Proceedings of the National Academy of Sciences*, vol. 115, no. 44, pp. E10467–E10475, 2018.
- [24] R. Aljundi, *Continual Learning in Neural Networks*. PhD thesis, KU Leuven, 2019.
- [25] G. I. Parisi, R. Kemker, J. L. Part, C. Kanan, and S. Wermter, "Continual lifelong learning with neural networks: A review," *Neural Networks*, vol. 113, pp. 54–71, 2019.
- [26] R. Grosse and J. Martens, "A kronecker-factored approximate fisher matrix for convolution layers," in *ICML'16 Proceedings of the 33rd International Conference on International Conference on Machine Learning - Volume 48*, pp. 573–582, 2016.
- [27] J. Zhang, D. Zhou, and M. Chen, "Monitoring multimode processes: a modified PCA algorithm with continual learning ability," *Journal of Process Control*, vol. 103, pp. 76–86, 2021.
- [28] M. Delange, R. Aljundi, M. Masana, S. Parisot, X. Jia, A. Leonardis, G. Slabaugh, and T. Tuytelaars, "A continual learning survey: Defying forgetting in classification tasks," *IEEE Transactions on Pattern Analysis and Machine Intelligence*, pp. 1–1, 2021.
- [29] R. Turner and M. Sahani, "A maximum-likelihood interpretation for slow feature analysis," *Neural Computation*, vol. 19, no. 4, pp. 1022–1038, 2007.
- [30] A. P. Dempster, N. M. Laird, and D. B. Rubin, "Maximum likelihood from incomplete data via the EM algorithm," *Journal of the royal*

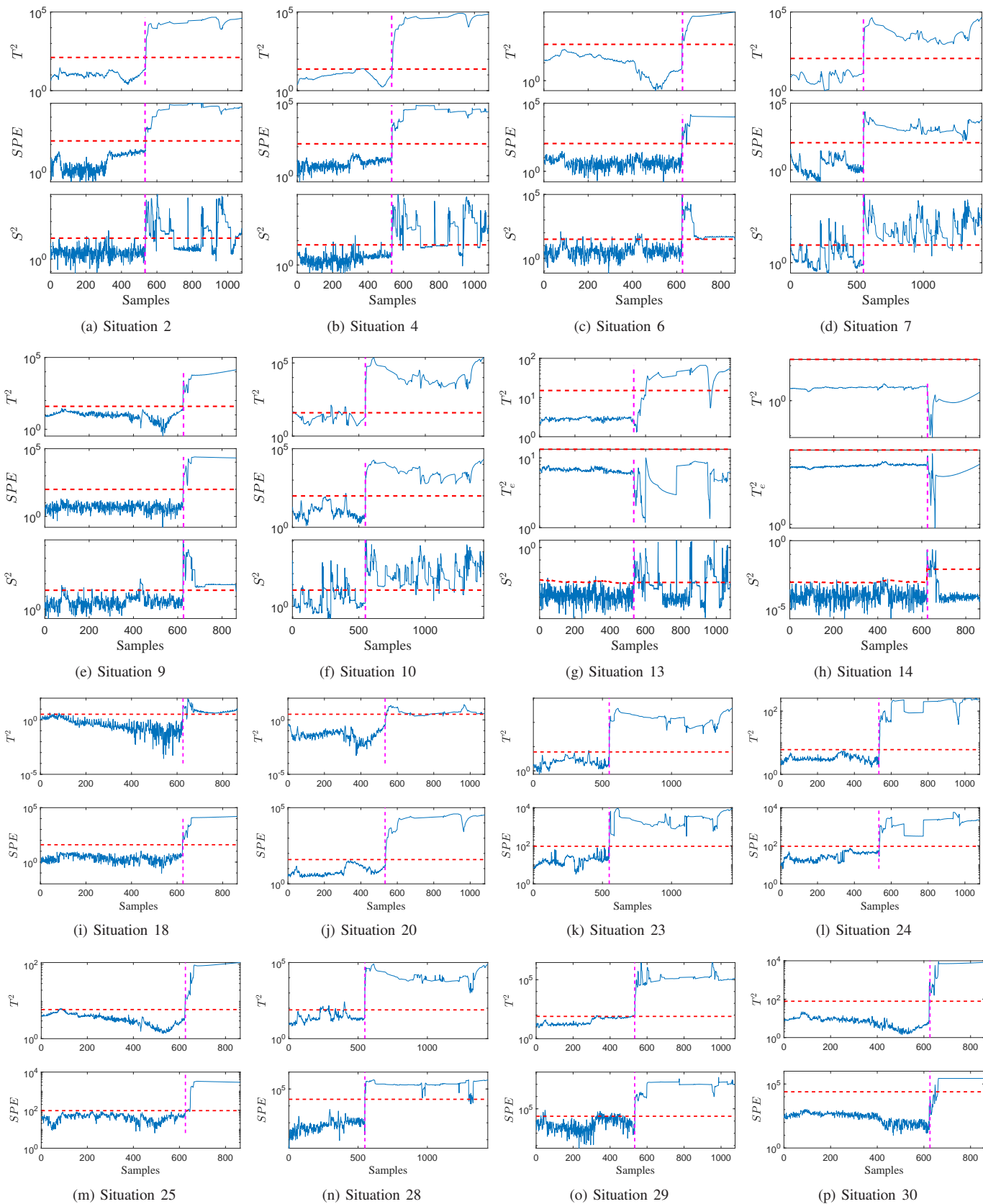


Fig. 4. Monitoring charts of Case 3

- statistical society series B-methodological*, vol. 39, no. 1, pp. 1–22, 1977.
- [31] F. Huszár, “On quadratic penalties in elastic weight consolidation,” *arXiv preprint arXiv:1712.03847*, 2017.
- [32] S. Sarkka, “Unscented rauch–tung–striebl smoother,” *IEEE Transactions on Automatic Control*, vol. 53, no. 3, pp. 845–849, 2008.
- [33] M. Quiñones-Grueiro, O. Llanes-Santiago, and A. J. S. Neto, *Monitoring Multimode Continuous Processes: A Data-Driven Approach*. Springer, 2020.
- [34] N. F. Thornhill, S. C. Patwardhan, and S. L. Shah, “A continuous stirred tank heater simulation model with applications,” *Journal of Process Control*, vol. 18, no. 3, pp. 347–360, 2008.
- [35] J. Martens, “New insights and perspectives on the natural gradient method,” *Journal of Machine Learning Research*, vol. 21, no. 146, pp. 1–76, 2020.